DFT Study on Retigerane-Type Sesterterpenoid Biosynthesis: Initial Conformation of GFPP Regulates Biosynthetic Pathway, Ring-Construction Order and Stereochemistry

Yuichiro Watanabe, Takahiro Hashishin, Hajime Sato,* Taro Matsuyama, Masaya Nakajima, Jun-ichi Haruta, and Masanobu Uchiyama*

ACCESS | 📊 Metrics & More | 📖 Article Recommendations | 🆘 Supporting Information

ABSTRACT: Retigerane-type sesterterpenoids, which feature a unique 5/6/5/5/5 fused pentacyclic structure with an angular-type triquinane moiety, are biosynthesized via successive carbocation-mediated reactions triggered by terpene cyclases. However, the precise biosynthetic pathways/mechanisms, wherein steric inversion of the carbon skeleton occurs at least once, remain elusive. Two plausible reaction pathways have been proposed, which differ in the order of ring cyclization: A → B/C → D/E-ring(s) (Route 1) and A → E → B → C/D-ring(s) (Route 2). Since the reaction intermediates of these complicated domino-type reaction sequences are experimentally inaccessible, we employed comprehensive density functional theory (DFT) calculations to evaluate these routes. The results indicate that retigeranin biosynthesis proceeds via Route 2 involving a multistep carbocation cascade, in which the order of ring cyclization (A → E → B → C/D) is the key to constructing the angular 5/5/5 triquinane structure with the correct stereochemistry at C3. The result also suggests that slight differences in the initial conformation have a significant effect on the order of cyclization and steric inversion. The computed pathway/mechanism also provides a rational basis for the formation of various related terpenes/terpenoids.

KEYWORDS: terpene, density functional theory, biosynthesis, rearrangement, carbocation, ring strain
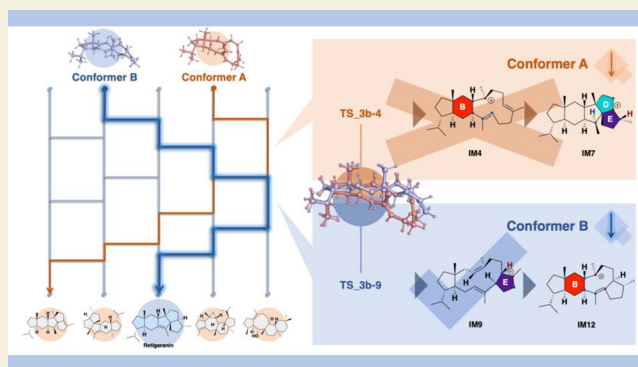
R etigeranic acid, a retigerane-type sesterterpenoid, has a unique fused pentacyclic skeleton with eight stereocenters, including three all-carbon quaternary (4°) centers, of which one is a bridgehead spirocenter. It was first isolated in 1965 from the Himalayan lichen *Lobaria retigera*,[1] and its structure was fully determined in 1972 by Shibata and co-workers,[2,3] who determined the X-ray crystal structure of the *p*-bromoanilide derivative.[4,5] In 1991, two stereoisomers ((−)-retigeranic acid A (*S* configuration at C18) and (−)-retigeranic acid B (*R* configuration at C18)) were identified using X-ray crystallography, again by Shibata.[6] The unique structure of retigeranic acid has attracted widespread attention,[7,8] and a number of synthetic studies on retigeranic acid have been reported.[9−13] In contrast, there have been few reports on its biosynthesis, though two plausible biosynthetic pathways have been proposed (Scheme 1).[2,14,15] Shibata and co-workers proposed Route 1.[2] In this route, dissociation of the pyrophosphate of geranylfarnesyl diphosphate (**GFPP**) and sequential annulations (A-ring formation) yield a 5/15 bicyclic intermediate (**i**), which undergoes 1,5-hydrogen (H) shift to afford an allylic carbocation (**ii**). From intermediate **ii**, B/C-ring formation proceeds to give a tetracyclic tertiary (3°)

cation (**iii**). Subsequently, deprotonative olefination of **iii** occurs to afford a neutral diene **iv**, which undergoes protonation of the C6−C7 π bond, leading to annulation to construct the D/E-rings via the formation of a 2° carbocation. However, protonation of the neutral olefin would require high energy, and such a deprotonation/protonation process appears to be unnecessary. Instead, Oikawa and co-workers suggested Route 2 based on their labeling experiments with ${}^{13}C/{}^{2}H$,[15] and they indicated that multiple H shifts at C6, C10, and C12 were involved in the biosynthetic cyclization process. Route 1 proposed by Shibata does not involve loss of the hydrogen at C6, which is inconsistent with the labeling experiment. Notably, the order of cyclization in the two pathways is quite different. In Route 2, the E-ring is formed first from

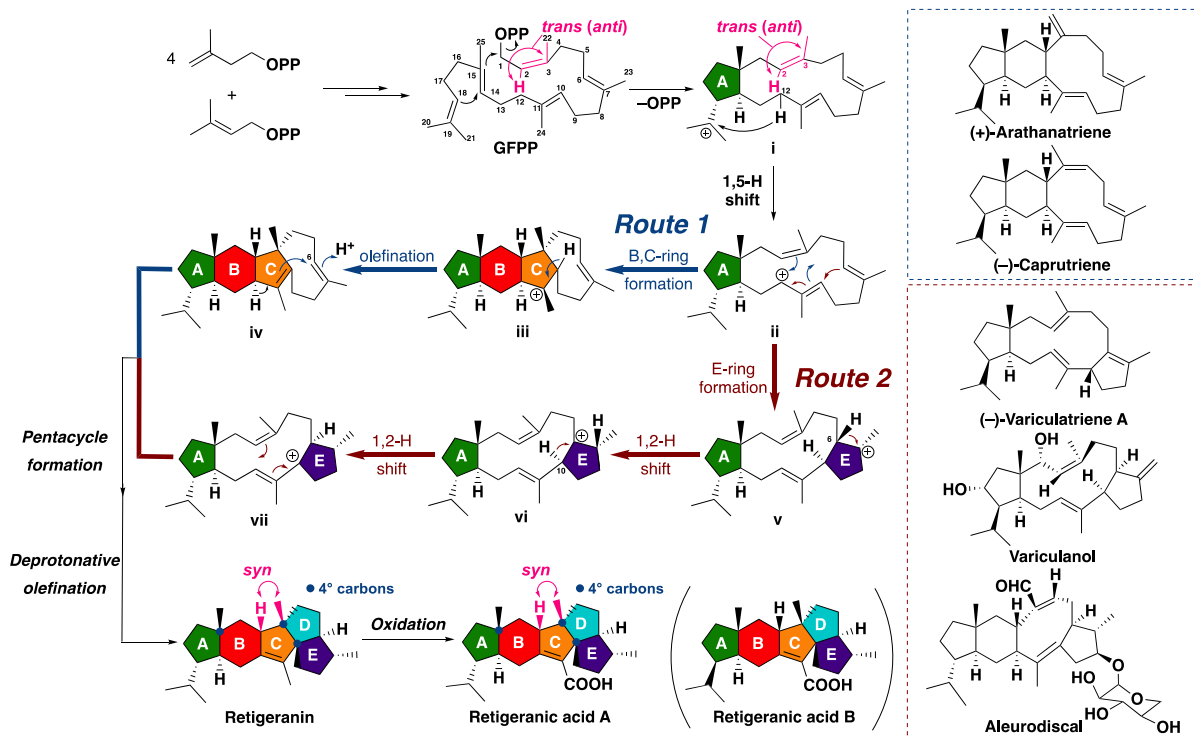**Scheme 1. Two Proposed Biosynthetic Pathways of (−)-Retigeranic Acid A**

intermediate **ii**, and then the B-, C-, and D-rings are constructed successively. However, the real biosynthetic pathway has not been determined. In which order does the ring formation take place? Another important point is the stereochemistry in the cyclization cascade: the hydrogen at the C2 position and the C3 methyl group are originally located on opposite sides (*trans*) of the double bond of **GFPP**, whereas they adopt the *syn* stereochemistry in the final product, indicating that a *syn/anti*-steric isomerization occurs somewhere during the cyclization cascade. However, the details of the isomerization mechanism/timing/reason remain unknown and have not been discussed in the literature.

Sesterterpene/terpenoids are fascinating compounds due to their complicated and diverse structures with a wide range of bioactivities, and some of their unique biosynthetic mechanisms have recently been elucidated.[16−21] In general, mechanistic issues in terpene biosynthesis are extremely difficult to resolve fully by means of experimental studies alone, since terpene cyclization is a domino-type reaction occurring inside a single enzyme ("black box"). However, pioneering work by various researchers, including Hess and Tantillo, has established the possible involvement of various types of carbocations, such as allyl cations, tertiary cations, secondary cations, and nonclassical cations, in the biosynthetic pathways of terpenes like lanosterol and pupukeanane.[22−34] Building on that, we have recently established a powerful combination of quantum-chemical calculations with the global reaction route mapping (GRRM) method[35,36] to unveil complicated biosynthetic pathways/mechanisms, such as those leading to sesterfisherol,[37] trichobrasilenol,[38] verrucosan,[39] and mangicol.[39] In particular, by combining computational and experimental techniques, we have successfully settled several long-standing controversies concerning the roles of different types of carbocations in several biosynthetic pathways.[37−39] In the present paper, we employ quantum

chemical calculations to uncover the details of retigeranin/retigeranic acid biosynthesis. The aims of the study are as follows: (i) to unveil the whole reaction pathway of the exquisitely controlled multistep biosynthetic carbocation-cascade reactions; and (ii) to elucidate the mechanism of the skeletal rearrangements/H shifts/conformational changes that afford the complicated, chiral, congested, polycyclic structure.

We first conducted kinetic/thermodynamic analysis of B/C-ring formation vs E-ring formation from the 5/15 bicyclic intermediate (**ii**), but obtained no definitive result (*vide infra*). Therefore, we conducted a systematic search of reaction pathways **IM1** → **IM8** by applying the retro-biosynthetic theoretical analysis strategy[40] (Scheme 2). The dissociation of pyrophosphate from **GFPP** initiates the multistep carbocation cascade and yields an allylic carbocation (**IM1**). Then, two successive cyclizations at C1−C15 and C14−C18 give the bicyclic 3° carbocation **IM2** with a 5/15 fused ring system (the A-ring is formed). Subsequently, a 1,5-H shift from C12 to C19 proceeds to yield **IM3**, followed by a conformational change in preparation for the next annulations. The reaction pathway from **IM1** to **IM3** appears to be similar for Route 1 and Route 2. In Route 1, the formation of the B-ring takes place prior to that of the E-ring. The allylic carbocation in **IM3b** is partially stabilized by a distal C2−C3 double bond and is thus conformationally more favorable than **IM3a** by 4.1 kcal mol^{-1}. Such cation-π interaction enables smooth formation of the B-ring with a small activation energy of 3.2 kcal mol^{-1}, giving a tricyclic 5/6/11 fused-ring intermediate **IM4**. This transformation changes the C2−C3 double bond (up to **IM3**) to a single bond with the 3° cation at C3. Thus, at **IM4**, the C3 stereogenic center can be geometrically inverted. This isomerization requires a relatively high energy of 23.2 kcal mol^{-1} to afford **IM5a**. After a conformational change to **IM5b**, C3−C10 annulation (C-ring formation) proceeds with an activation energy of 14.2 kcal mol^{-1} to give the 5/6/5/8

Scheme 2. Results of DFT Evaluation of Two Proposed Biosynthetic Pathways of Retigeranin[a]
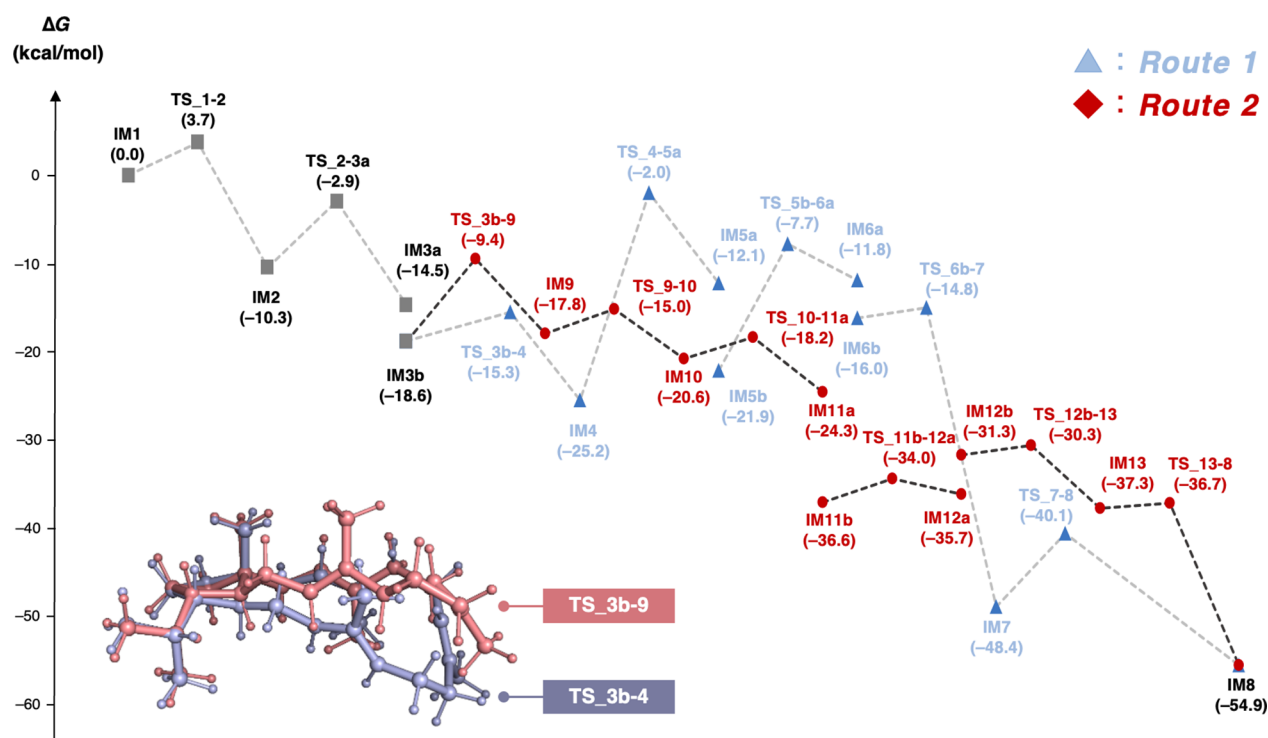

A. Route 1
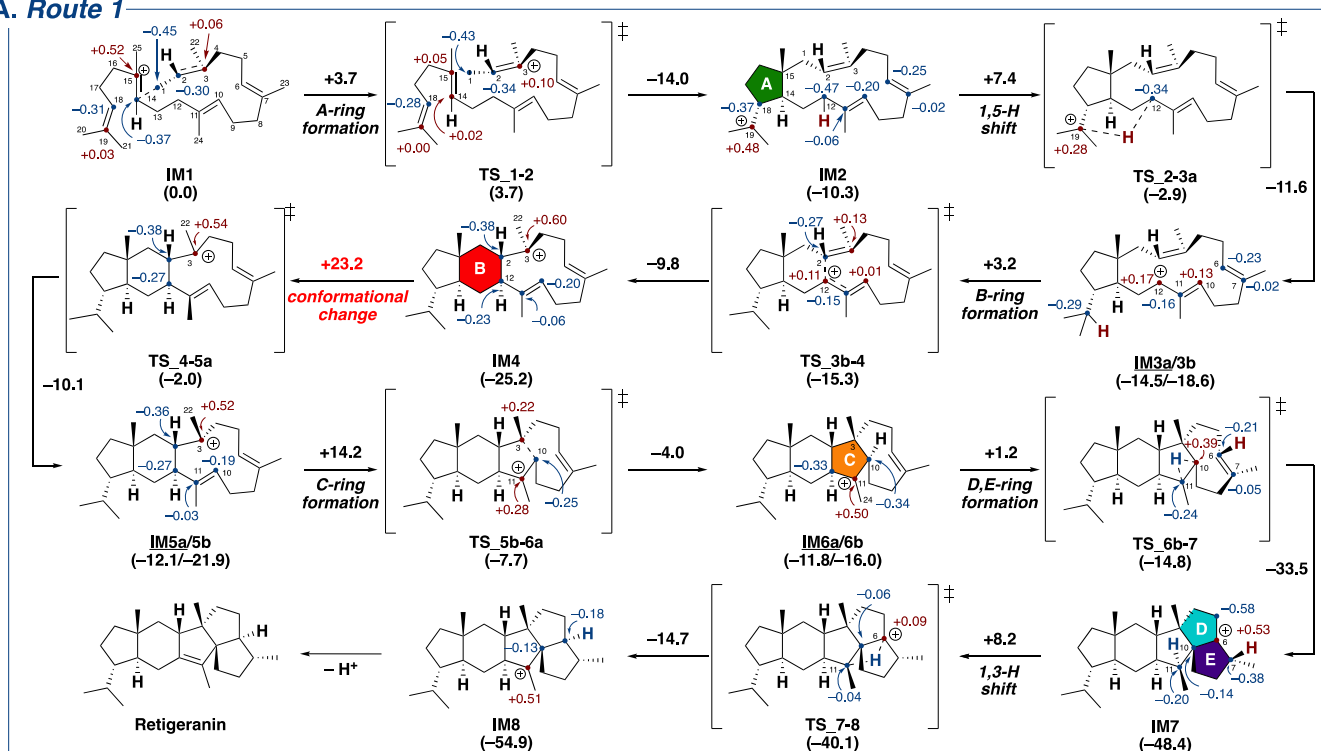
B. Route 2
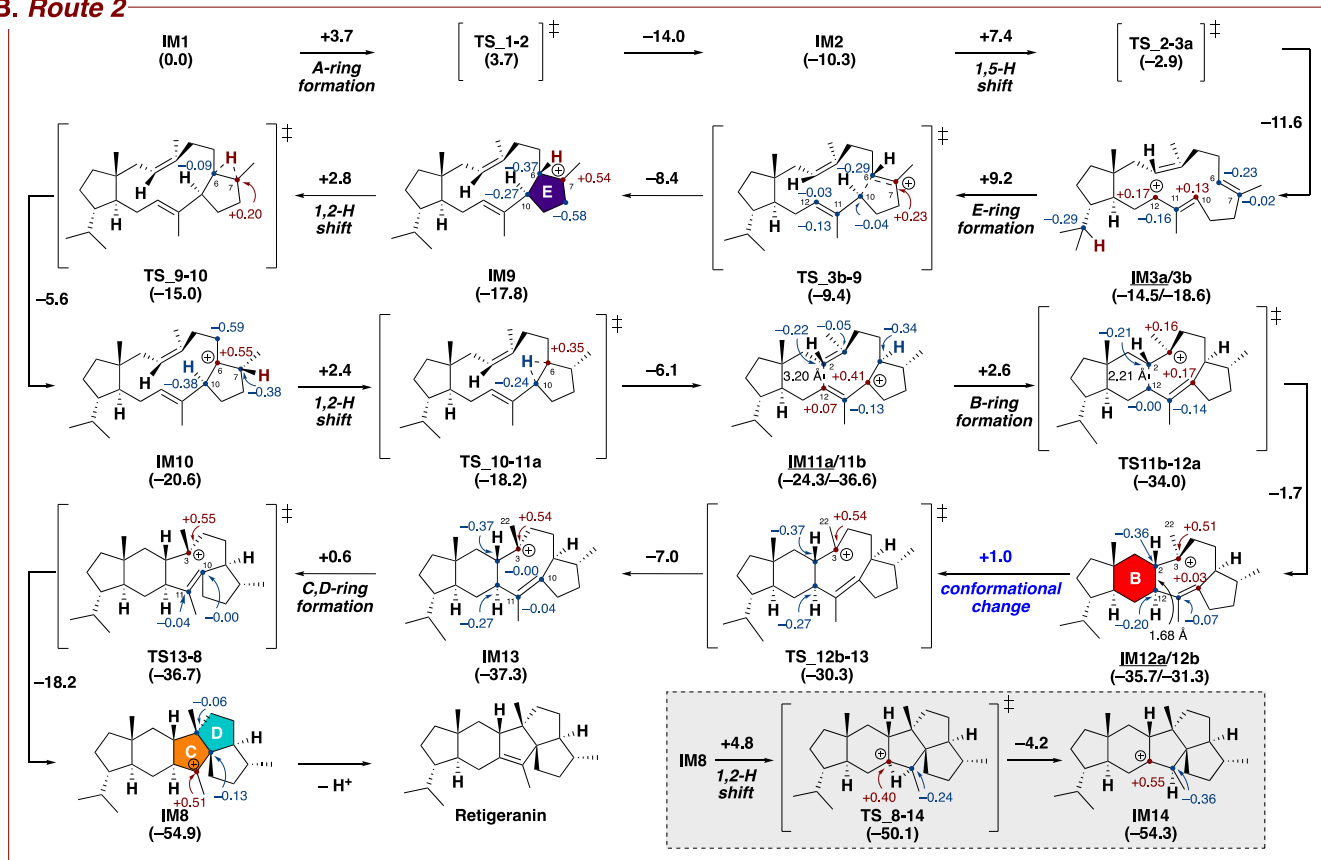
[a]If there are **IM**s with different conformations, they are grouped together (structural information is given only for the underlined **IM**s). Numbers indicate electronic charges on key carbon atoms (indicated by curved arrows where necessary for clarity). Potential energies (kcal mol^{-1}, Gibbs free energies calculated at the M06-2X/6-311+G(d,p) based on M06-2X/6-31+G(d,p) geometries) relative to the neighboring intermediates are shown on above the arrows. **IM**, intermediate; **TS**, transition state.

Figure 1. Computed potential energy profiles for Route 1 (in light blue) and Route 2 (in red). Potential energies (kcal mol^{-1}, Gibbs free energies calculated at the M06-2X/6-311+G(d,p) based on M06-2X/6-31+G(d,p) geometries) relative to **IM1a** are shown in parentheses. **IM**, intermediate; **TS**, transition state.

tetracyclic 3° carbocation intermediate **IM6a**. As the conformation of **IM6a** changes to afford **IM6b** with small exothermicity, the double 1,2-H shifts and C6−C10 annulation (D/E-ring formation) occur concertedly with a small activation energy of only 1.2 kcal mol^{-1}, affording the bridgehead 3° carbocation **IM7** with large exothermicity (33.5 kcal mol^{-1}). A close examination of the IRC (intrinsic reaction coordinate) calculation suggests that this step includes three chemical processes; (i) the hydride shifts from C10 to C11 first to afford a bridgehead 3° cation at C10, followed by (ii) C6−C10 σ bond formation (D/E-ring formation), and finally (iii) another hydride shifts from C6 to C7 to afford another bridgehead 3° cation at C6 (**IM7**). Subsequently, 1,3-H shift from C11 to C6 proceeds with an activation barrier of 8.2 kcal mol^{-1} to give a more stable 3° carbocation **IM8**. Finally, deprotonation affords the product, retigeranin (possibly via the bridgehead 3° carbocation **IM14**). We also investigated other possible reaction pathways, including successive deprotonative olefination and proton-catalyzed annulation (Scheme 1, **iv**) as originally considered by Shibata, but we could not locate any other route with reasonable activation energies. Consequently, we propose the pathway from **IM1a** to **IM8** as a modification of Route 1 that can also rationalize all H-shifts including that at C6 suggested by the results of labeling experiments by Oikawac and co-workers (Scheme 2A).

Next, we will discuss Route 2, in which the E-ring is formed first. In Route 2, from **IM3b**, E-ring formation proceeds through a cation-π interaction with the distal C6−C7 double bond to give a tricyclic 5/12/5 fused-ring intermediate **IM9** with an activation barrier of 9.2 kcal mol^{-1}. A close examination of the transition structure analysis revealed that

the conformations of **TS_3b-4** (Route 1) and **TS_3b-9** (Route 2) are different, suggesting a difference in the shape of the substrate-binding pocket or in the binding mode to the pocket (Figure 1). Next, two successive 1,2-H shifts via **TS_9-10** and **TS_10-11a** proceed with very small activation barriers to give **IM11a**. After a conformational change from **IM11a** to **IM11b** that is exothermic (12.3 kcal mol^{-1}) partly due to effective interaction of the allyl cation with the distal C2−C3 π electrons, B-ring formation (C2−C12 annulation) takes place smoothly to yield the 3° cation **IM12a**. Then, a conformational change to **IM12b** followed by *syn/anti*-interconversion at C3 proceeds with barriers of only 4.4 and 1.0 kcal mol^{-1}, respectively, affording **IM13**. This conformational change proceeds smoothly to eliminate distortion of the 8-membered ring. Thus, cation-mediated C3−C10 bond formation affords the pentacyclic intermediate **IM8** with the characteristic angular triquinane structure, which undergoes deprotonation (olefination) to give the product, retigeranin. This computed Route 2 is in good agreement with the results of labeling experiments by Oikawa and co-workers, and the energy diagram (Figure 1) suggests a thermodynamically and kinetically favorable biosynthetic reaction cascade: (1) the activation barriers are all low enough for the reactions to proceed smoothly at ambient temperature, (2) the entire energy profile descends as the reactions proceed, and (3) the overall exothermicity is very large. On the other hand, Route 1 appears to be relatively energetically unfavorable around the steric inversion from **IM4**.
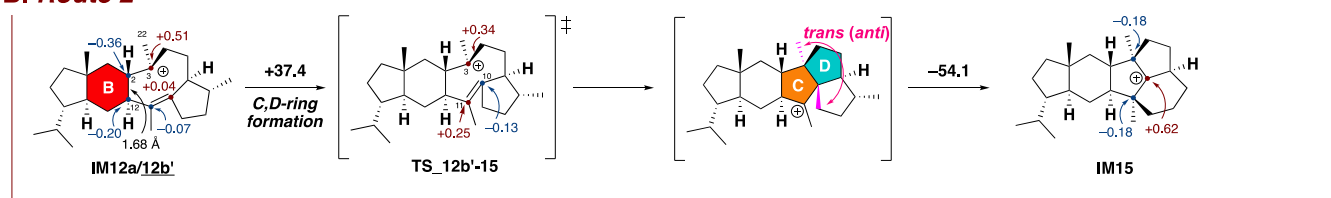
Thus, we next focused on the reason why *trans-cis* isomerization occurs in the biosynthesis of retigeranin. In Route 2, we successfully located an artificial annulation route

Scheme 3. Results of DFT Evaluation of Two Pathways without Steric Inversion[a]
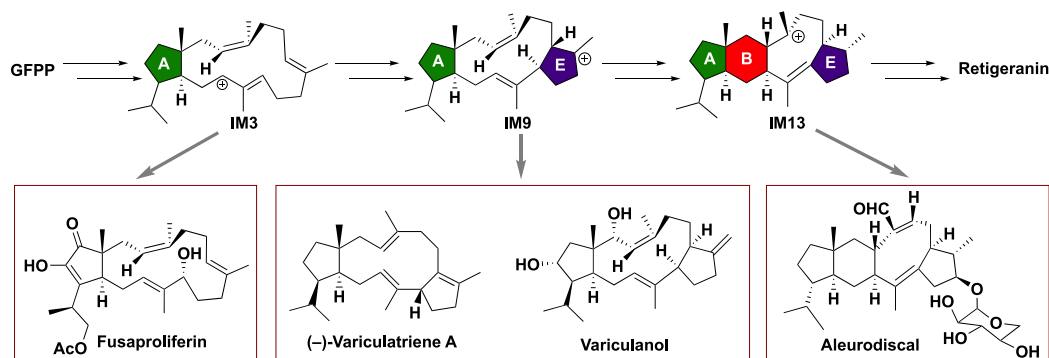

A. Route 1'
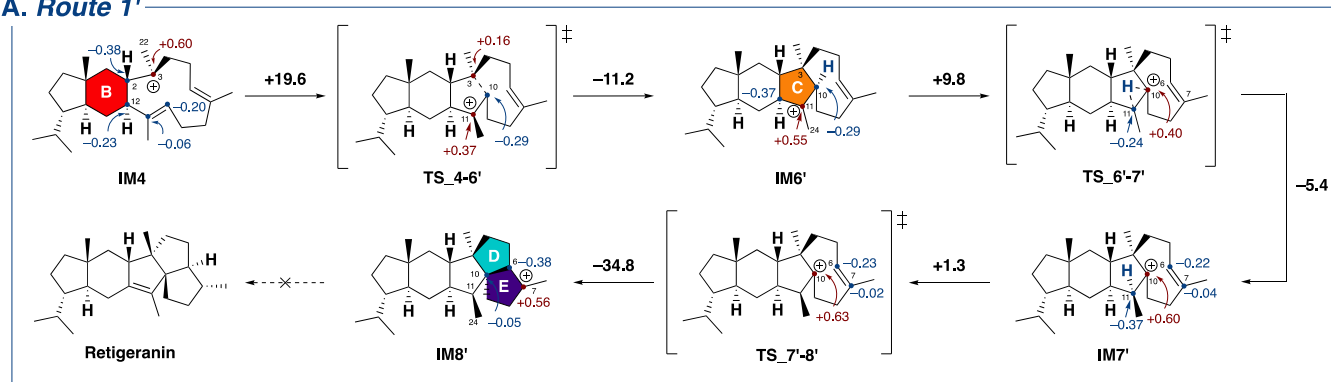
B. Route 2'

[a]Potential energies (kcal mol^{-1}, Gibbs free energies calculated at the M06-2X/6-311+G(d,p) based on M06-2X/6-31+G(d,p) geometries) relative to the neighboring intermediates are shown above the arrows. **IM**, intermediate; **TS**, transition state.

Scheme 4. Sesterterpenoid Analogues Branching from Our Proposed Biosynthetic Pathway

from **IM12** without the steric interconversion at C3 (Scheme 3B) on the potential energy surface (PES), but (**i**) it would be necessary to overcome a very high activation energy (>37 kcal mol^{-1}), and (**ii**) the resulting 5/5/5 triquinane 3° cation at C11 would undergo a smooth ring expansion without an energy barrier to afford another 5/5/6 tricyclo structure (**IM15**) along the intrinsic reaction coordinate (IRC). This is consistent with the fact that trans-5/5-ring junctions are generally difficult.[40] Thus, we confirmed that the conformational change (**IM12 → IM13**) in Route 2, required to construct the retigeranin structure, is the most kinetically favored pathway. On the contrary, in Route 1, the C-ring formation with retention of the stereochemistry of C3 (Scheme 3A, **IM4 → IM6'**) turned out to be kinetically more favorable than the bond rotation (syn/anti isomerization route) (Scheme 2A, **IM4 → IM5 → IM6**). Note that this retention route gives another 5/6/5/5/5 retigeranin skeleton (**IM8'**) with a very different stereochemistry and carbocation. On the basis of the above discussion, we can conclude that the biosynthesis of retigerane-type sesterterpenoids proceeds through Route 2 and that the initial conformation of **GFPP**

is critical not only for the order of ring construction, but also for the stereochemistry.[41,42] Notably, the computed pathway/mechanism of Route 2 also provides a rational basis for the formation of related terpenes/terpenoids (Scheme 4). On the basis of the **IM**s on the computed Route 2, it appears that fusaproliferin[43] and variculatriene/variculanol[44] can be biosynthesized from **IM3** and **IM9**, respectively, and **IM13** serves as an intermediate for the biosynthesis of aleurodiscal.[45] Thus, the results obtained in this study not only provide an overall picture of the biosynthesis of retigeranin/retigeranic acid, but also suggest that the reaction pathway would be applicable to various other retigerane-type sesterterpenoids. In light of the present computational results, the active site of the cyclase may show some flexibility. However, it remains unclear how the initial conformation is fixed in the terpene cyclase's active site. Recently, Osbourne and co-workers identified a terpene cyclase that is responsible for retigeranic acid production from *A. thaliana* by applying a genome mining strategy.[46] Moreover, Wang and Zhang and co-workers identified important residues for (−)-retigeranin production by comparing TPS19 and TPS18 mutants.[47] However, the roles of the

mutated residues remain unclear. By combining our computational results with these experimental results, it may be possible to elucidate the mechanism generating the initial conformation for terpene biosynthesis.

In summary, we have uncovered the mechanistic details of retigerane-type sesterterpenoid biosynthesis, as well as providing new insight into the key role of the ring-construction order in determining the stereochemistries during the synthesis of the 5/6/5/5/5 angular triquinane skeleton. In particular, we clarified the exquisite skeletal reconstruction processes and conformational changes (the Cartesian coordinates of the 3D structures of all species are given in the Supporting Information). Future comparative study of the terpene cyclases responsible for fusaproliferin, variculanol, and aleurodiscal formation could help to establish the molecular basis of regulation of the branching biosynthetic pathways.[48,49] We believe that our findings should be helpful for future mechanistic studies and also for engineering of terpene/terpenoid biosynthesis.

■ METHODS

All calculations were carried out using the Gaussian 16 program package,[50] and GRRM17, GRRM23[35,36] program. Structure optimizations were performed at the M06-2X level[51] in the gas phase using the 6-31+G(d,p) basis set. The vibrational frequencies were computed at the same level to check whether each optimized structure is an energy minimum (no imaginary frequency) or a transition state (one imaginary frequency) and to evaluate its zero-point vibrational energy (ZPVE) and thermal corrections at 298 K. Intrinsic reaction coordinates (IRC)[52−55] were calculated to confirm the connection between the transition states and the reactants/products. Single-point energies were calculated at the M06-2X/6-311+G(d,p) based on the structures optimized by the M06-2X/6-31+G(d,p) method. The Gibbs free energy used for discussion in this study was calculated by adding the gas-phase Gibbs free energy correction.

■ ASSOCIATED CONTENT

ⓈⓁ Supporting Information

The Supporting Information is available free of charge at https://pubs.acs.org/doi/10.1021/jacsau.4c00313.

Computational details, 3D representation of the structure, coordinates and energies for all computed structures (PDF)

■ AUTHOR INFORMATION

Corresponding Authors

Hajime Sato — *Graduate School of Pharmaceutical Sciences, The University of Tokyo, Bunkyo-ku, Tokyo 113-0033, Japan; Interdisciplinary Graduate School of Medicine and Engineering, University of Yamanashi, Kofu, Yamanashi 400-8510, Japan;* ⓞ orcid.org/0000-0001-5185-096X; Email: hsato@yamanashi.ac.jp

Masanobu Uchiyama — *Graduate School of Pharmaceutical Sciences, The University of Tokyo, Bunkyo-ku, Tokyo 113-0033, Japan; Research Initiative for Supra-Materials (RISM), Shinshu University, Ueda, Nagano 386-8567, Japan;* ⓞ orcid.org/0000-0001-6385-5944; Email: uchiyama@mol.f.u-tokyo.ac.jp

Authors

Yuichiro Watanabe — *Graduate School of Pharmaceutical Sciences, The University of Tokyo, Bunkyo-ku, Tokyo 113-0033, Japan; Graduate School of Pharmaceutical Sciences, Osaka University, Suita-shi, Osaka 565-0871, Japan*

Takahiro Hashishin — *Graduate School of Pharmaceutical Sciences, The University of Tokyo, Bunkyo-ku, Tokyo 113-0033, Japan*

Taro Matsuyama — *Graduate School of Pharmaceutical Sciences, The University of Tokyo, Bunkyo-ku, Tokyo 113-0033, Japan*

Masaya Nakajima — *Graduate School of Pharmaceutical Sciences, The University of Tokyo, Bunkyo-ku, Tokyo 113-0033, Japan*

Jun-ichi Haruta — *Graduate School of Pharmaceutical Sciences, Osaka University, Suita-shi, Osaka 565-0871, Japan*

Complete contact information is available at:
https://pubs.acs.org/10.1021/jacsau.4c00313

Author Contributions

CRediT: **Yuichiro Watanabe** data curation, investigation, writing-original draft; **Takahiro Hashishin** data curation, investigation; **Hajime Sato** conceptualization, data curation, formal analysis, funding acquisition, project administration, validation, writing-review & editing; **Taro Matsuyama** data curation, validation, visualization, writing-review & editing; **Masaya Nakajima** validation, visualization, writing-review & editing; **Junichi Haruta** writing-review & editing; **Masanobu Uchiyama** conceptualization, funding acquisition, project administration, resources, supervision, writing-review & editing.

Notes

The authors declare no competing financial interest.

■ REFERENCES

(1) Rao, P. S.; Sarma, K. G.; Seshadri, T. R. Chemical Components of The Lobaria Lichens from the Western Himalayas. *Curr. Sci.* **1965**, *34* (1), 9−11.

(2) Kaneda, M.; Takahashi, R.; Iitaka, Y.; Shibata, S. Retigeranic Acid, a Novel Sesterterpene Isolated from the Lichens of Group. *Tetrahedron Lett.* **1972**, *13* (45), 4609−4611.

(3) Takahashi, R.; Chiang, H. C.; Aimi, N.; Tanaka, O.; Shibata, S. The Structures of Retigeric Acids A and B from Lichens of the Lobaria Retigera Group. *Phytochemistry* **1972**, *11* (6), 2039−2045.

(4) Takahashi, R.; Iitaka, Y. The Crystal and Molecular Structure of P-Bromophenacyl Retigerate A. *Acta Crystallogr. Sect. B Struct. Crystallogr. Cryst. Chem.* **1972**, *28* (3), 764−770.

(5) Kaneda, M.; Iitaka, Y.; Shibata, S. X-Ray Studies of C 25 Terpenoids. IV. The Crystal Structure of Retigeranic Acid p -Bromoanilide. *Acta Crystallogr. Sect. B Struct. Crystallogr. Cryst. Chem.* **1974**, *30* (2), 358–364.

(6) Sugawara, H.; Kasuya, A.; Iitaka, Y.; Shibata, S. Further Studies on the Structure of Retigeranic Acid. *Chem. Pharm. Bull.* **1991**, *39* (11), 3051–3054.

(7) Mehta, G.; Srikrishna, A. Synthesis of Polyquinane Natural Products: An Update. *Chem. Rev.* **1997**, *97* (3), 671–719.

(8) Hog, D. T.; Webster, R.; Trauner, D. Synthetic Approaches toward Sesterterpenoids. *Nat. Prod. Rep.* **2012**, *29* (7), 752.

(9) Han, Y.; Breitler, S.; Zheng, S.-L.; Corey, E. J. Enantioselective Conversion of Achiral Cyclohexadienones to Chiral Cyclohexenones by Desymmetrization. *Org. Lett.* **2016**, *18* (23), 6172–6175.

(10) Breitler, S.; Han, Y.; Corey, E. J. Highly Diastereoselective Cationic Cyclization Reactions Convert a Common Monocyclic Enone to Bicyclic Precursors for the Synthesis of Retigeranic Acids A and B. *Org. Lett.* **2017**, *19* (24), 6686–6687.

(11) Wang, X.; Li, D.; Zhang, J.; Gong, J.; Fu, J.; Yang, Z. A Synthetic Route to The Core Structure of (−)-Retigeranic Acid A. *Org. Lett.* **2021**, *23* (13), 5092–5097.

(12) Sun, D.; Chen, R.; Tang, D.; Xia, Q.; Zhao, Y.; Liu, C.-H.; Ding, H. Total Synthesis of (−)-Retigeranic Acid A: A Reductive Skeletal Rearrangement Strategy. *J. Am. Chem. Soc.* **2023**, *145* (22), 11927–11932.

(13) Chen, X.; Yao, W.; Zheng, H.; Wang, H.; Zhou, P.-P.; Zhu, D.-Y.; Wang, S.-H. Enantiocontrolled Total Synthesis of (−)-Retigeranic Acid A. *J. Am. Chem. Soc.* **2023**, *145* (25), 13549–13555.

(14) Millot, M.; Martin-De-Lassalle, M.; Chollet-Krugler, M.; Champavier, Y.; Mambu, L.; Chulia, J. A.; Lacaille-Dubois, M. A. Two New Retigerane-Type Sesterterpenoids from the Lichen Leprocaulon Microscopicum. *Helv. Chim. Acta* **2016**, *99* (2), 169–173.

(15) Ye, Y.; Minami, A.; Mandi, A.; Liu, C.; Taniguchi, T.; Kuzuyama, T.; Monde, K.; Gomi, K.; Oikawa, H. Genome Mining for Sesterterpenes Using Bifunctional Terpene Synthases Reveals a Unified Intermediate of Di/Sesterterpenes. *J. Am. Chem. Soc.* **2015**, *137* (36), 11846–11853.

(16) Huang, A. C.; Hong, Y. J.; Bond, A. D.; Tantillo, D. J.; Osbourn, A. Diverged Plant Terpene Synthases Reroute the Carbocation Cyclization Path towards the Formation of Unprecedented 6/11/5 and 6/6/7/5 Sesterterpene Scaffolds. *Angew. Chem., Int. Ed.* **2018**, *57* (5), 1291–1295.

(17) Guo, J.; Cai, Y. S.; Cheng, F.; Yang, C.; Zhang, W.; Yu, W.; Yan, J.; Deng, Z.; Hong, K. Genome Mining Reveals a Multiproduct Sesterterpenoid Biosynthetic Gene Cluster in Aspergillus Ustus. *Org. Lett.* **2021**, *23* (5), 1525–1529.

(18) Quan, Z.; Hou, A.; Goldfuss, B.; Dickschat, J. S. Mechanism of the Bifunctional Multiple Product Sesterterpene Synthase AcAS from Aspergillus Calidoustus. *Angew. Chem., Int. Ed.* **2022**, *61* (13), No. e202117273.

(19) Gu, B.; Goldfuss, B.; Dickschat, J. S. Mechanistic Character-isation and Engineering of Sesterviolene Synthase from Streptomyces Violens. *Angew. Chem., Int. Ed.* **2023**, *62* (1), No. e202215688.

(20) Gu, B.; Goldfuss, B.; Schnakenburg, G.; Dickschat, J. S. Subrutilane—A Hexacyclic Sesterterpene from Streptomyces Sub-rutilus. *Angew. Chem., Int. Ed.* **2023**, *62* (48), No. e202313789.

(21) Xu, H.; Schnakenburg, G.; Goldfuss, B.; Dickschat, J. S. Mechanistic Characterisation of the Bacterial Sesterviridene Synthase from Kitasatospora Viridis. *Angew. Chem., Int. Ed.* **2023**, *62* (31), No. e202306429.

(22) Tantillo, D. J. The Carbocation Continuum in Terpene Biosynthesis—Where Are the Secondary Cations? *Chem. Soc. Rev.* **2010**, *39* (8), 2847–2854.

(23) Chen, N.; Wang, S.; Smentek, L.; Hess, B. A.; Wu, R. Biosynthetic Mechanism of Lanosterol: Cyclization. *Angew. Chem., Int. Ed.* **2015**, *54* (30), 8693–8696.

(24) Hess, B. A.; Smentek, L. The Concerted Nature of the Cyclization of Squalene Oxide to the Protosterol Cation. *Angew. Chem., Int. Ed.* **2013**, *52* (42), 11029–11033.

(25) Hess, B. A.; Smentek, L.; Noel, J. P.; O'Maille, P. E. Physical Constraints on Sesquiterpene Diversity Arising from Cyclization of the Eudesm-5-Yl Carbocation. *J. Am. Chem. Soc.* **2011**, *133* (32), 12632–12641.

(26) Smentek, L.; Hess, B. A. Compelling Computational Evidence for the Concerted Cyclization of the ABC Rings of Hopene from Protonated Squalene. *J. Am. Chem. Soc.* **2010**, *132* (48), 17111–17117.

(27) Hong, Y. J.; Tantillo, D. J. How Many Secondary Carbocations Are Involved in the Biosynthesis of Avermitilol? *Org. Lett.* **2011**, *13* (6), 1294–1297.

(28) McCulley, C. H.; Tantillo, D. J. Secondary Carbocations in the Biosynthesis of Pupukeanane Sesquiterpenes. *J. Phys. Chem. A* **2018**, *122* (40), 8058–8061.

(29) Zev, S.; Gupta, P. K.; Pahima, E.; Major, D. T. A Benchmark Study of Quantum Mechanics and Quantum Mechanics-Molecular Mechanics Methods for Carbocation Chemistry. *J. Chem. Theory Comput.* **2022**, *18* (1), 167–178.

(30) Dixit, M.; Weitman, M.; Gao, J.; Major, D. T. Chemical Control in the Battle against Fidelity in Promiscuous Natural Product Biosynthesis: The Case of Trichodiene Synthase. *ACS Catal.* **2017**, *7* (1), 812–818.

(31) Raz, K.; Levi, S.; Gupta, P. K.; Major, D. T. Enzymatic Control of Product Distribution in Terpene Synthases: Insights from Multiscale Simulations. *Curr. Opin. Biotechnol.* **2020**, *65*, 248–258.

(32) Ansbacher, T.; Freud, Y.; Major, D. T. Slow-Starter Enzymes: Role of Active-Site Architecture in the Catalytic Control of the Biosynthesis of Taxadiene by Taxadiene Synthase. *Biochemistry* **2018**, *57* (26), 3773–3779.

(33) Dixit, M.; Weitman, M.; Gao, J.; Major, D. T. Substrate Folding Modes in Trichodiene Synthase: A Determinant of Chemo- and Stereoselectivity. *ACS Catal.* **2018**, *8* (2), 1371–1375.

(34) Zhang, F.; Wang, Y.; Yue, J.; Zhang, R.; Hu, Y. e.; Huang, R.; Ji, A. j.; Hess, B. A.; Liu, Z.; Duan, L.; Wu, R. Discovering a Uniform Functional Trade-off of the CBCtype 2,3-Oxidosqualene Cyclases and Deciphering Its Chemical Logic. *Sci. Adv.* **2023**, *9* (23), No. eadh1418.

(35) Maeda, S.; Harabuchi, Y.; Sumiya, Y.; Takagi, M.; Suzuki, K.; Hatanaka, M.; Osada, Y.; Taketsugu, T.; Morokuma, K.; Ohno, K. *GRRM17, GRRM23*, see http://iqce.jp/GRRM/index_e.shtml (accessed date 22 12, 2023).

(36) Maeda, S.; Ohno, K.; Morokuma, K. Systematic Exploration of the Mechanism of Chemical Reactions: The Global Reaction Route Mapping (GRRM) Strategy Using the ADDF and AFIR Methods. *Phys. Chem. Chem. Phys.* **2013**, *15* (11), 3683–3701.

(37) Sato, H.; Narita, K.; Minami, A.; Yamazaki, M.; Wang, C.; Suemune, H.; Nagano, S.; Tomita, T.; Oikawa, H.; Uchiyama, M. Theoretical Study of Sesterfisherol Biosynthesis: Computational Prediction of Key Amino Acid Residue in Terpene Synthase. *Sci. Rep.* **2018**, *8* (1), 2473.

(38) Sato, H.; Hashishin, T.; Kanazawa, J.; Miyamoto, K.; Uchiyama, M. DFT Study of a Missing Piece in Brasilane-Type Structure Biosynthesis: An Unusual Skeletal Rearrangement. *J. Am. Chem. Soc.* **2020**, *142* (47), 19830–19834.

(39) Sato, H.; Li, B.-X.; Takagi, T.; Wang, C.; Miyamoto, K.; Uchiyama, M. DFT Study on the Biosynthesis of Verrucosane Diterpenoids and Mangicol Sesterterpenoids: Involvement of Secondary-Carbocation-Free Reaction Cascades. *JACS Au* **2021**, *1* (8), 1231–1239.

(40) Matsuyama, T.; Togashi, K.; Nakano, M.; Sato, H.; Uchiyama, M. Revision of the Peniroquesine Biosynthetic Pathway by Retro-Biosynthetic Theoretical Analysis: Ring Strain Controls the Unique Carbocation Rearrangement Cascade. *JACS Au* **2023**, *3* (6), 1596–1603.

(41) In our previous study, we demonstrated the importance of the initial conformation, in determining the outcome of the carbocation cascade, see: Sato, H.; Mitsuhashi, T.; Yamazaki, M.; Abe, I.;

Uchiyama, M. Computational Studies on Biosynthetic Carbocation Rearrangements Leading to Quiannulatene: Initial Conformation Regulates Biosynthetic Route, Stereochemistry, and Skeleton Type. *Angew. Chem., Int. Ed.* **2018**, *57* (45), 14752−14757.

(42) Sakamoto, K.; Sato, H.; Uchiyama, M. DFT Study on the Biosynthesis of Asperterpenol and Preasperterpenoid Sesterterpenoids: Exclusion of Secondary Carbocation Intermediates and Origin of Structural Diversification. *J. Org. Chem.* **2022**, *87* (9), 6432−6437.

(43) Santini, A.; Ritieni, A.; Fogliano, V.; Randazzo, G.; Mannina, L.; Logrieco, A.; Benedetti, E. Structure and Absolute Stereochemistry of Fusaproliferin, a Toxic Metabolite from Fusarium Proliferatum. *J. Nat. Prod.* **1996**, *59* (2), 109−112.

(44) Singh, S. B.; Reamer, R. A.; Zink, D.; Schmatz, D.; Dombrowski, A.; Goetz, M. A. Variculanol: Structure and Absolute Stereochemistry of a Novel 5/12/5 Tricyclic Sesterterpenoid from Aspergillus Variecolor. *J. Org. Chem.* **1991**, *56* (19), 5618−5622.

(45) Lauer, U.; Anke, T.; Sheldrick, W. S.; Scherer, A.; Steglich, W. ANTIBIOTICS FROM BASIDIOMYCETES XXXI. ALEURODISCAL: AN ANTIFUNGAL SESTERTERPENOID FROM ALEURODISCUS MIRABILIS (BERK. & CURT.) HÖHN. *J. Antibiot. (Tokyo)* **1989**, *42* (6), 875−882.

(46) Huang, A. C.; Kautsar, S. A.; Hong, Y. J.; Medema, M. H.; Bond, A. D.; Tantillo, D. J.; Osbourn, A. Unearthing a Sesterterpene Biosynthetic Repertoire in the Brassicaceae through Genome Mining Reveals Convergent Evolution. *Proc. Natl. Acad. Sci. U. S. A.* **2017**, *114* (29), E6005−E6014.

(47) Chen, Q.; Li, J.; Liu, Z.; Mitsuhashi, T.; Zhang, Y.; Liu, H.; Ma, Y.; He, J.; Shinada, T.; Sato, T.; Wang, Y.; Liu, H.; Abe, I.; Zhang, P.; Wang, G. Molecular Basis for Sesterterpene Diversity Produced by Plant Terpene Synthases. *Plant Commun.* **2020**, *1* (5), No. 100051.

(48) Minami, A.; Ozaki, T.; Liu, C.; Oikawa, H. Cyclopentane-Forming Di/Sesterterpene Synthases: Widely Distributed Enzymes in Bacteria, Fungi, and Plants. *Nat. Prod. Rep.* **2018**, *35* (12), 1330−1346.

(49) Quan, Z.; Hou, A.; Goldfuss, B.; Dickschat, J. S. Mechanism of the Bifunctional Multiple Product Sesterterpene Synthase AcAS from *Aspergillus calidoustus*. *Angew. Chem., Int. Ed.* **2022**, *61* (13), No. e202117273.

(50) Frish, M. J. et al. *Gaussian 16 Revision C.01*; Gaussian, Inc: Wallingford CT, 2016. Full citations are given in Supporting Information.

(51) Zhao, Y.; Truhlar, D. G. The M06 suite of density functionals for main group thermochemistry, thermochemical kinetics, non-covalent interactions, excited states, and transition elements: two new functionals and systematic testing of four M06-class functionals and 12 other functionals. *Theor. Chem. Acc.* **2008**, *120*, 215−241.

(52) Fukui, K. The path of chemical reactions - the IRC approach. *Acc. Chem. Res.* **1981**, *14*, 363−368.

(53) Page, M.; Doubleday, C.; McIver, J. W., Jr Following steepest descent reaction paths. The use of higher energy derivatives with *ab initio* electronic structure methods. *J. Chem. Phys.* **1990**, *93*, 5634−5642.

(54) Ishida, K.; Morokuma, K.; Komornicki, A. The intrinsic reaction coordinate. An *ab initio* calculation for HNCHCN and H⁻+CH₄→CH₄+H⁻. *J. Chem. Phys.* **1977**, *66*, 2153−2156.

(55) Gonzalez, C.; Schlegel, H. B. Reaction path following in mass-weighted internal coordinates. *J. Phys. Chem.* **1990**, *94*, 5523−5527.